Electronic Supplementary Material (ESI) for RSC Advances.

Supporting Information

Selective sensing of Al^{3+} by napthyridine coupled rhodamine chemosensors

Kumaresh Ghosh*, Anupam Majumdar and Tanmay Sarkar
Department of Chemistry, University of Kalyani, Kalyani-741235, India;
Email: ghosh_k2003@yahoo.co.in

1. Change in emission of receptor 1 with various metal ions in MeCN/water (4/1, v/v; 10 µM tris HCl buffer; pH = 7).

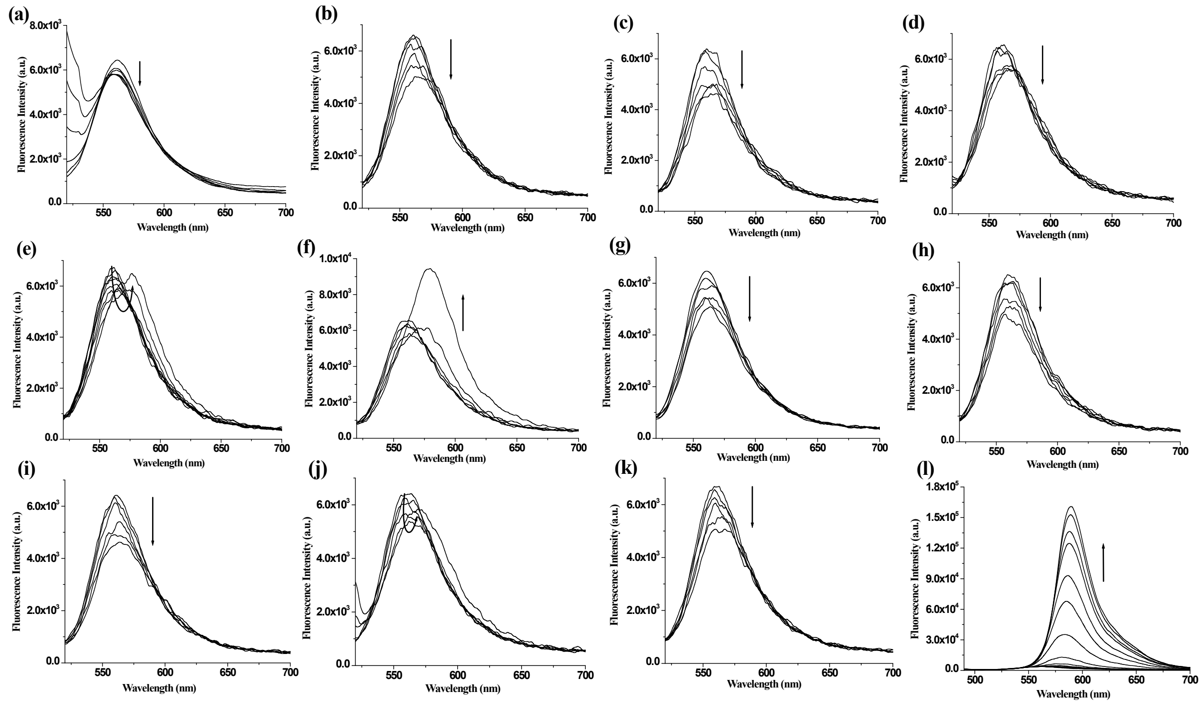

Figure S1. Emission titration spectra for **1** (c = 3 x 10^{-5} M, λ_{exc} = 510 nm) with ,(a) Ag^{+}, (b) Cd^{2+}, (c) Co^{2+}, (d) Cr^{3+}, (e) Cu^{2+}, (f) Fe^{3+}, (g) Hg^{2+}, (h) Mg^{2+}, (i) Ni^{2+}, (j) Pb^{2+}, (k) Zn^{2+} and (l) **1** (c = 3 x 10^{-5} M, λ_{exc} = 480) with Al^{3+} in MeCN/water (4/1,v/v; 10 µM tris HCl buffer; pH =7) (in all cases [cation] =1.2 x 10^{-3} M).

2. Change in emission of receptor 2 with various metal ions in MeCN/water (4/1, v/v; 10 µM tris HCl buffer; pH = 7).

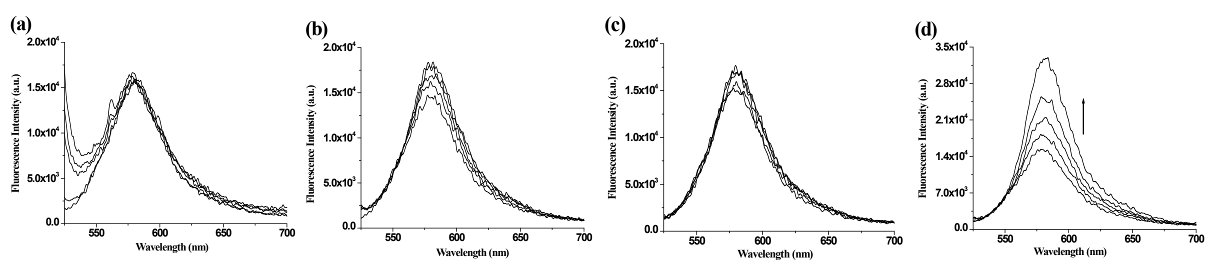

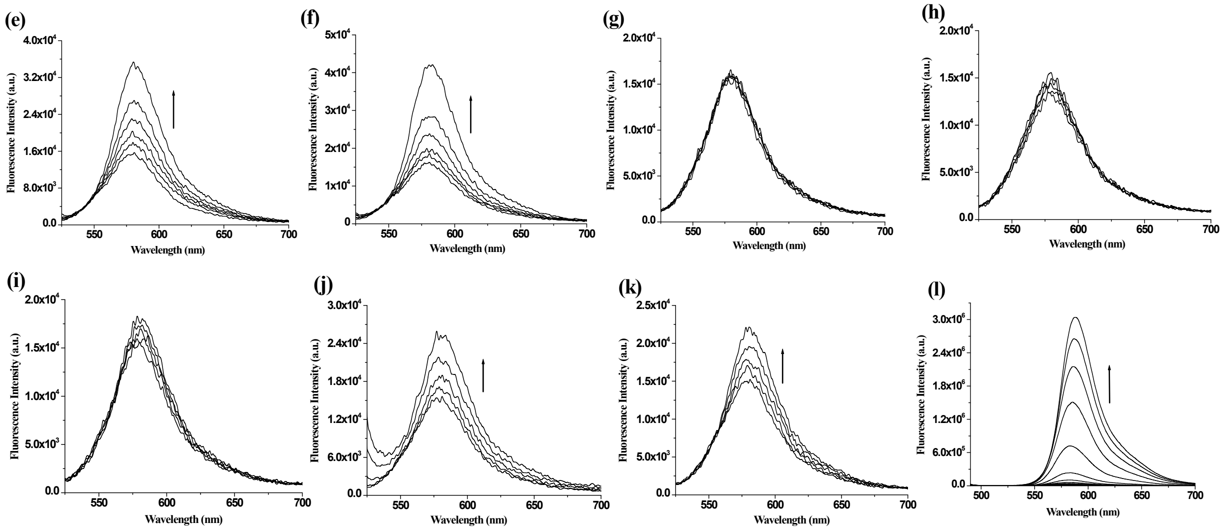

Figure S2. Emission titration spectra for **2** (c = 3 x 10^{-5} M, λ_{exc} = 510 nm) with (a) Ag^{+}, (b) Cd^{2+}, (c) Co^{2+}, (d) Cr^{3+}, (e) Cu^{2+}, (f) Fe^{3+}, (g) Hg^{2+}, (h) Mg^{2+}, (i) Ni^{2+}, (j) Pb^{2+}, (k) Zn^{2+} and (l) **2** (c = 3 x 10^{-5} M, λ_{exc} = 480 nm) with Al^{3+} in MeCN/water (4/1,v/v; 10 μM tris HCl buffer; pH =7) (in all cases [cation] =1.2 x 10^{-3} M).

3. Change in absorbance of receptor 1 with various metal ions in MeCN/water (4/1, v/v; 10 μM tris HCl buffer; pH = 7).

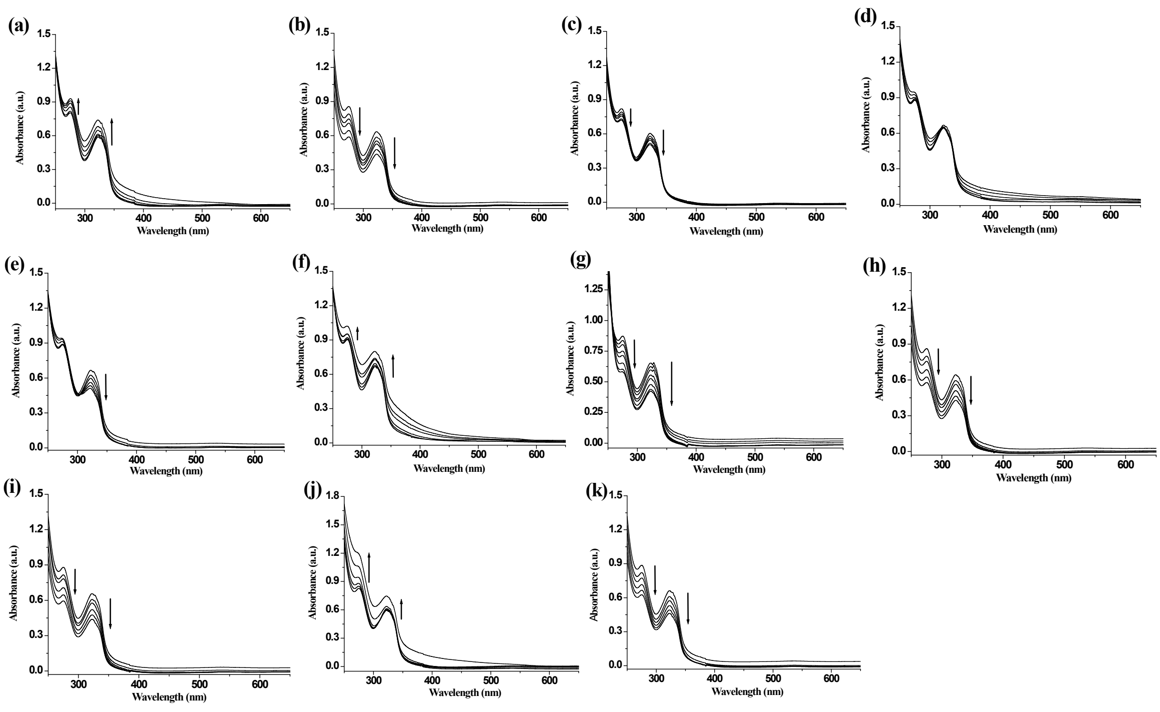

Figure S3. Absorption titration spectra for **1** (c = 3 x 10^{-5} M) with ,(a) Ag^{+}, (b) Cd^{2+}, (c) Co^{2+}, (d) Cr^{3+}, (e) Cu^{2+}, (f) Fe^{3+}, (g) Hg^{2+}, (h) Mg^{2+}, (i) Ni^{2+}, (j) Pb^{2+} and (k) Zn^{2+} in MeCN/water (4/1,v/v; 10 μM tris HCl buffer; pH =7) (in all cases [cation] =1.2 x 10^{-3} M).

4. Change in absorbance of receptor 2 with various metal ions in MeCN/water (4/1, v/v; 10 μM tris HCl buffer; pH = 7).

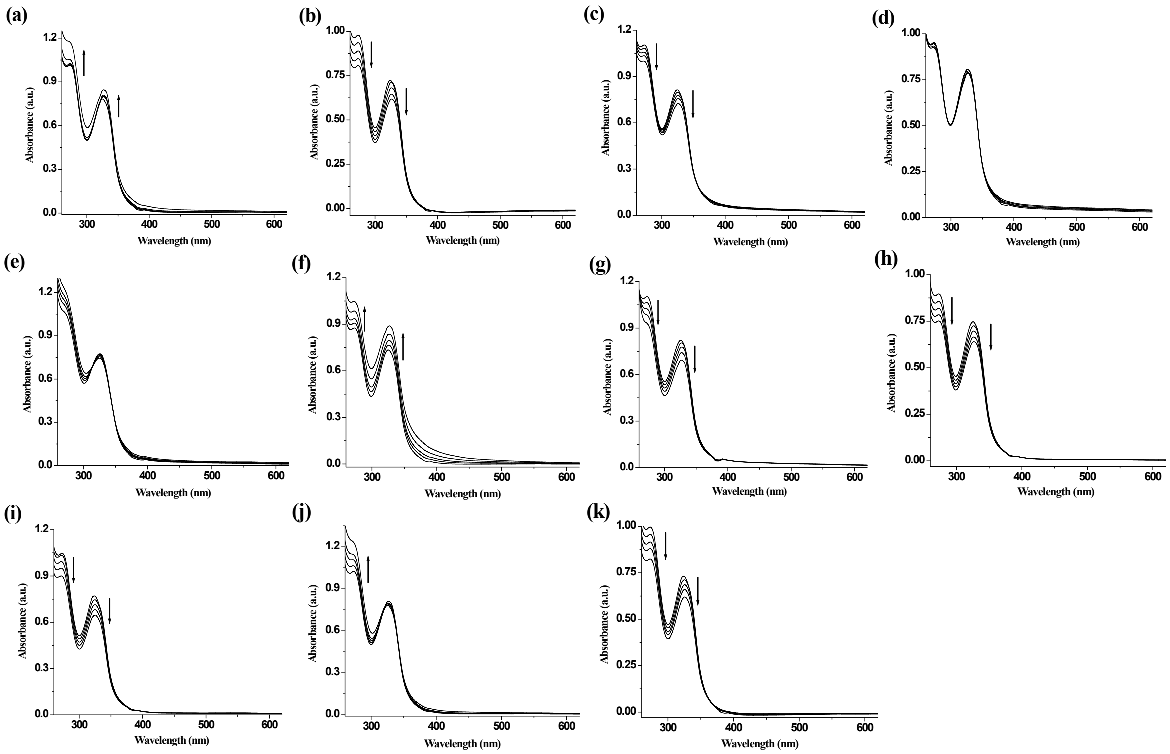

Figure S4. Absorption titration spectra for **2** (c = 3 x 10^{-5} M) with ,(a) Ag^{+}, (b) Cd^{2+}, (c) Co^{2+}, (d) Cr^{3+}, (e) Cu^{2+}, (f) Fe^{3+}, (g) Hg^{2+}, (h) Mg^{2+}, (i) Ni^{2+}, (j) Pb^{2+} and (k) Zn^{2+} in MeCN/water (4/1,v/v; 10 μM tris HCl buffer; pH =7) (in all cases [cation] =1.2 x 10^{-3} M).

5. Job plots of 1 and 2 with Al^{3+} ion.

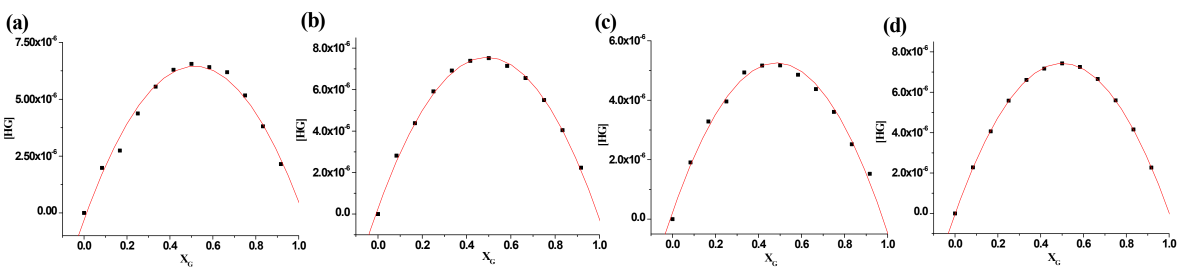

Figure S5. (a) Fluorescence and (b) Uv Job plots for **1** with Al^{3+} in MeCN/water (4/1,v/v; 10 μM tris HCl buffer; pH =7) ([H] = [G] = 3 × 10^{-5} M); (c) Fluorescence and (d) Uv Job plots for **2** with Al^{3+} in MeCN/water (4/1,v/v; 10 μM tris HCl buffer; pH =7) ([H] = [G] = 3 × 10^{-5} M).

6. Nonlinear curve fitting of the fluorescence titration data for 1 and 2 with Al^{3+} ion.

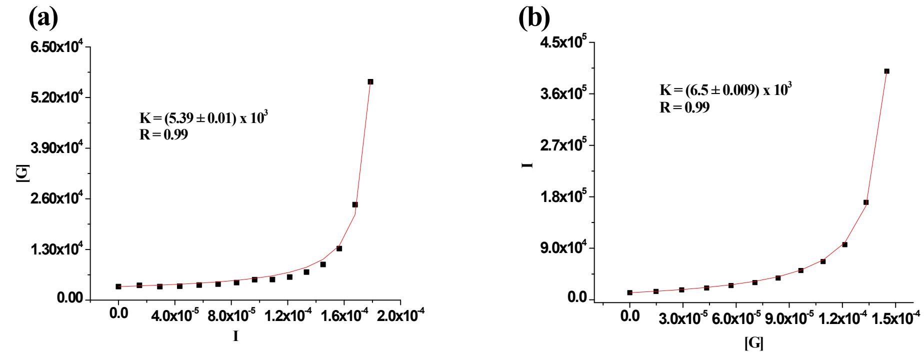

Figure S6. (a) Nonlinear curve fitting of the fluorescence titration data for **1**(c = 3 × 10^{-5} M) with Al^{3+} in MeCN/water (4/1,v/v; 10 μM tris HCl buffer; pH =7) upon addition of Al^{3+} and (b) Nonlinear curve fitting of the fluorescence titration data for **2**(c = 3 × 10^{-5} M) with Al^{3+} in MeCN/water (4/1,v/v; 10 μM tris HCl buffer; pH =7) upon addition of Al^{3+}.

Note: The nonlinear fit was done using equation (1)[1] where I represents the intensity; I_0 represents the intensity of pure host; C_H and C_G are corresponding concentration of host and cationic guest; Ka is the binding constant. The binding constant (Ka) and the correlation coefficient (R) were obtained from a nonlinear least-square analysis of I *vs* C_H and C_G.

$$I = I_0 + (I_{\lim} - I_0) / 2C_H \{C_H + C_G + 1/K_a - [(C_H + C_G + 1/K_a)^2 - 4C_HC_G]^{1/2}\} \qquad (1)$$

7. Detection limit for Al^{3+} ion.

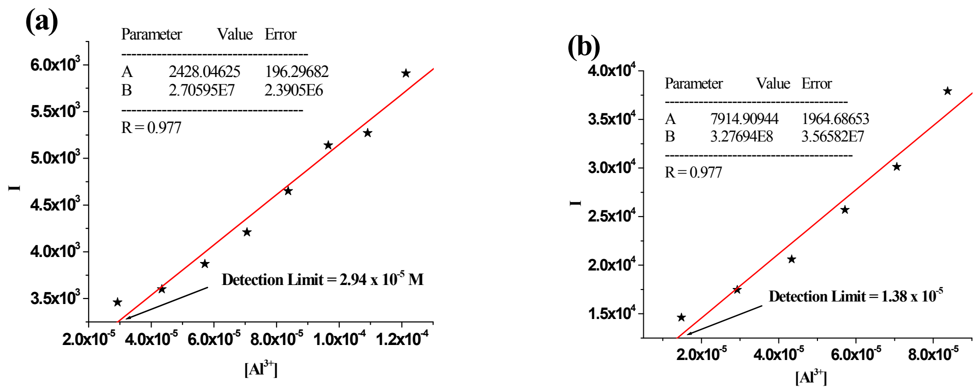

Figure S7: Plot for the evaluation of detection limit for Al^{3+} ion from fluorescence of (a) **1** and (b) **2**.

8. Change in absorbance and emission of 1 with $AlCl_3$ and K_2SO_4. $Al_2(SO_4)_3$. $24H_2O$ in MeCN/water (4/1, v/v; 10 μM tris HCl buffer; pH = 7).

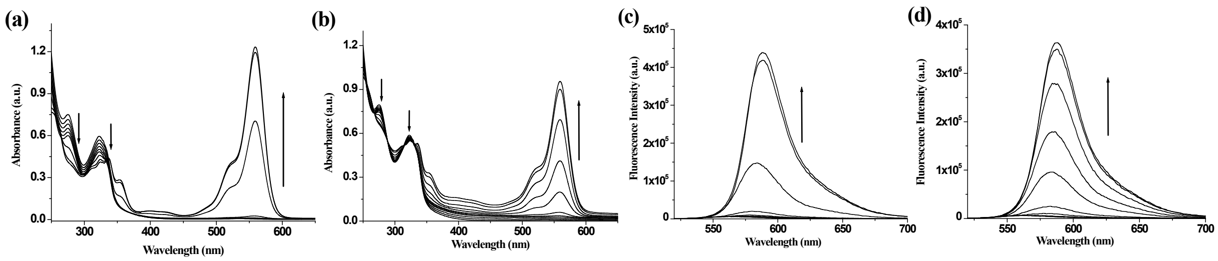

Figure S8. UV-vis titration spectra of (a) **1** (c = 3 x 10^{-5} M) upon addition of $AlCl_3$ (c = 1.2 x 10^{-3} M), (b) **1** (c = 3 x 10^{-5} M) upon addition of K_2SO_4. $Al_2(SO_4)_3$. $24H_2O$ (c = 1.2 x 10^{-3} M) in CH_3CN/water (4/1, v/v; 10 μM tris HCl, pH = 7.0); Fluorescence titration spectra of (c) **1** (c = 3 x 10^{-5} M) upon addition of $AlCl_3$ (c = 1.2 x 10^{-3} M) and (d) **1** (c = 3 x 10^{-5} M) upon addition of K_2SO_4. $Al_2(SO_4)_3$. $24H_2O$ (c = 1.2 x 10^{-3} M) in CH_3CN/water (4/1, v/v; 10 μM tris HCl, pH = 7.0).

9. Change in absorbance and emission of 2 with $AlCl_3$ and K_2SO_4. $Al_2(SO_4)_3$. $24H_2O$ in MeCN/water (4/1, v/v; 10 μM tris HCl buffer; pH = 7).

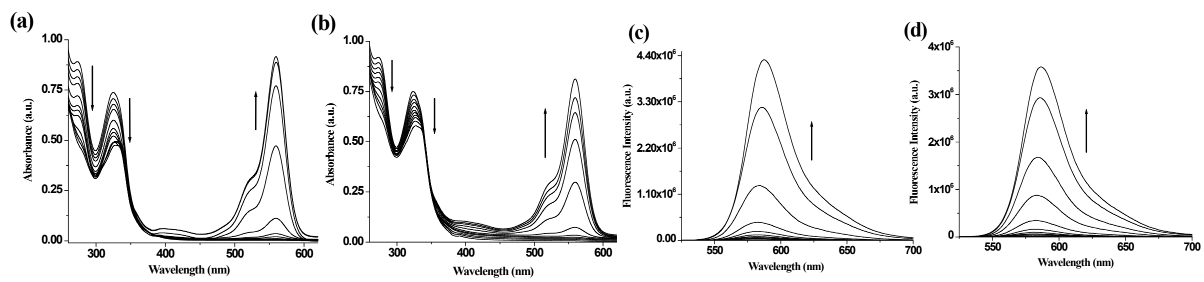

Figure S9. UV-vis titration spectra of (a) **2** (c = 3 x 10^{-5} M) upon addition of $AlCl_3$ (c = 1.2 x 10^{-3} M), (b) **2** (c = 3 x 10^{-5} M) upon addition of K_2SO_4. $Al_2(SO_4)_3$. $24H_2O$ (c = 1.2 x 10^{-3} M) in CH_3CN/water (4/1, v/v; 10 μM tris HCl, pH = 7.0); Fluorescence titration spectra of (c) **2** (c = 3 x 10^{-5} M) upon addition of $AlCl_3$ (c = 1.2 x 10^{-3} M) and (d) **2** (c = 3 x 10^{-5} M) upon addition of K_2SO_4. $Al_2(SO_4)_3$. $24H_2O$ (c = 1.2 x 10^{-3} M) in CH_3CN/water (4/1, v/v; 10 μM tris HCl, pH = 7.0).

10. Change in absorption and emission of 1.Al^{3+} and 2.Al^{3+} complex with F^- ions in MeCN/water (4/1, v/v; 10 μM tris HCl buffer; pH = 7).

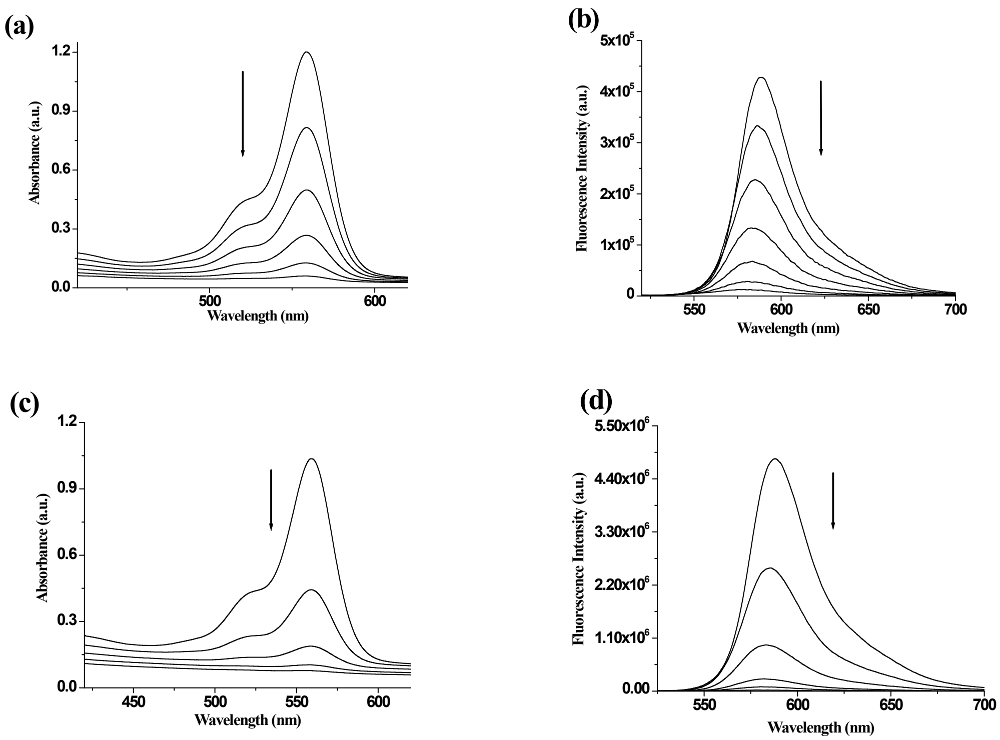

Figure S10. Changes (a) in absorbance and (b) emission of **1**-Al^{3+} complex in CH_3CN/H_2O (4/1, v/v; 10 μM tris HCl buffer; pH 7.0) upon addition of F^- ions ($c = 3 \times 10^{-3}$ M); Changes (c) in absorbance and (b) emission of **2**-Al^{3+} complex in CH_3CN/H_2O (4/1, v/v; 10 μM tris HCl buffer; pH 7.0) upon addition of F^- ions ($c = 3 \times 10^{-3}$ M).

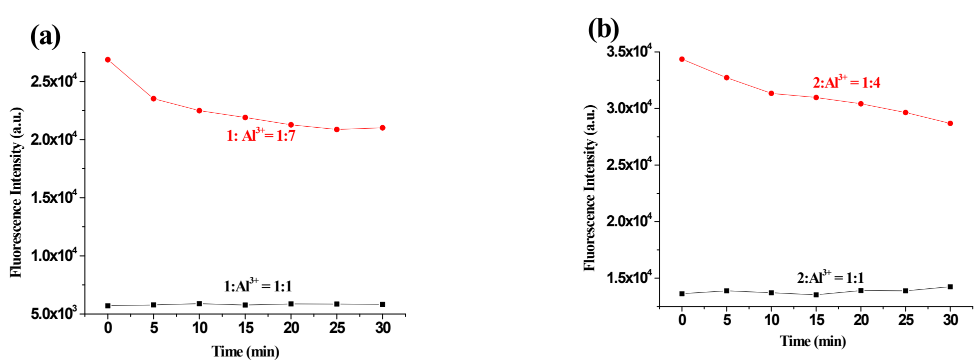

Figure S11. Change in emission of the Al-complexes of **1** and **2** in CH_3CN/H_2O (4/1, v/v; 10 μM tris HCl buffer; pH 7.0) with time.

11. ^{1}H NMR of 1 ($CDCl_3$ 400 MHz):

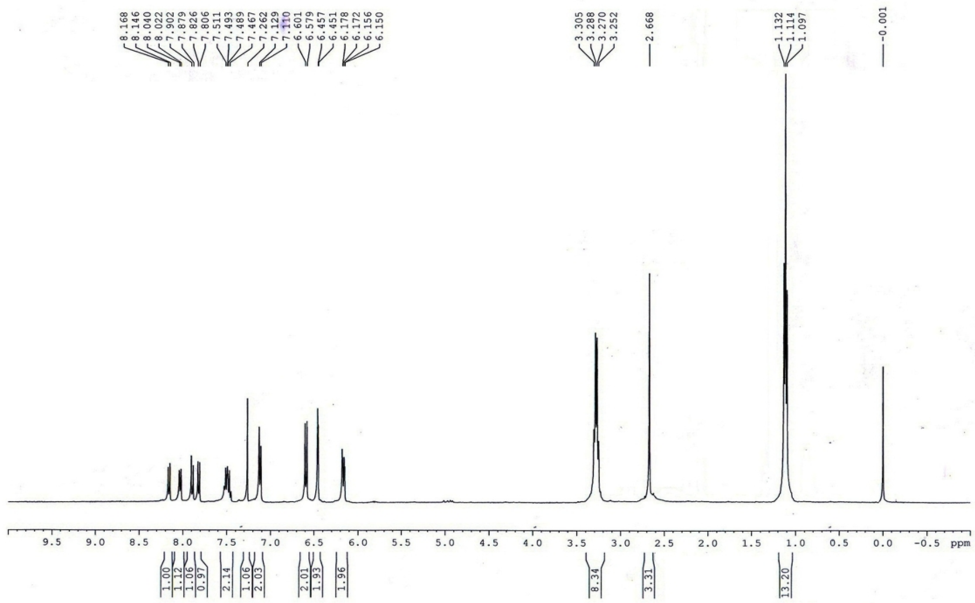

12. ^{13}C NMR of 1 ($CDCl_3$ 100 MHz):

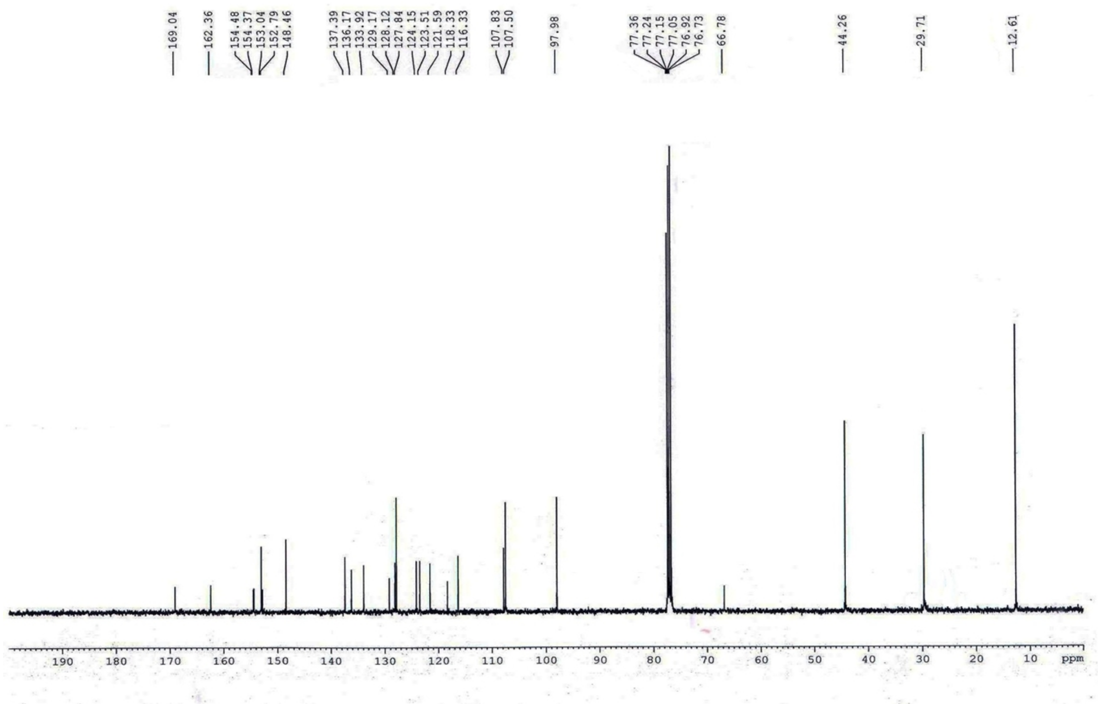

13. HRMS of 1:

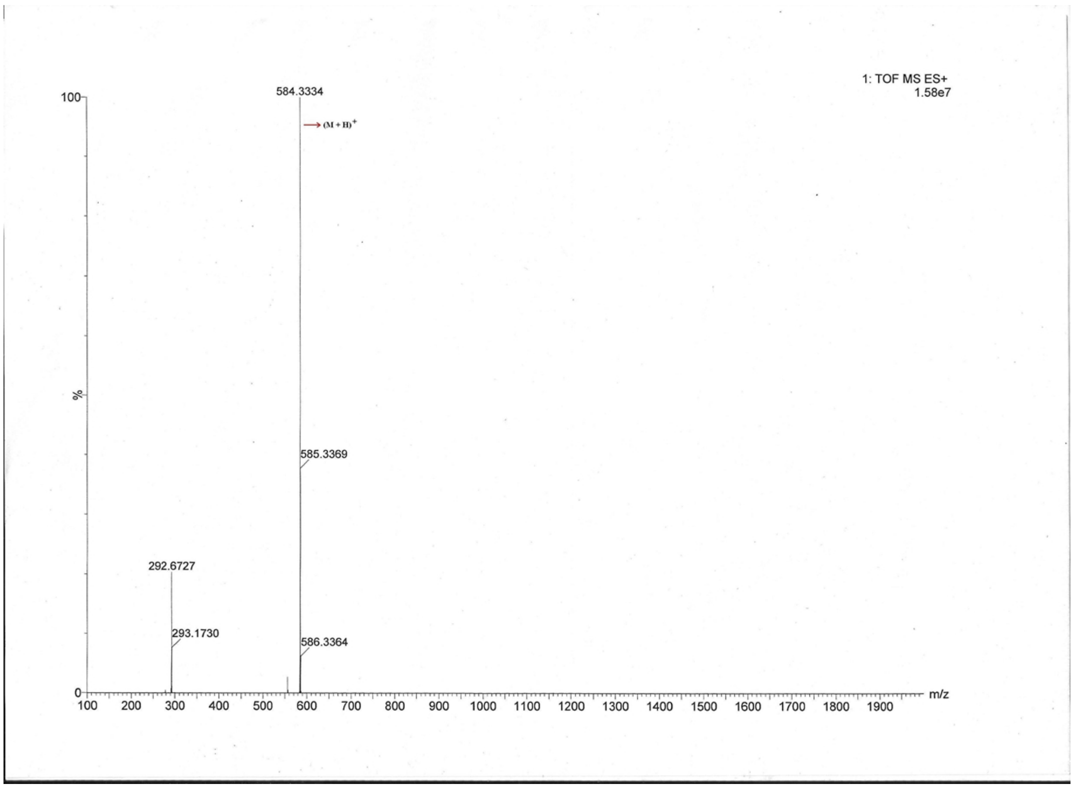

1: TOF MS ES+
1.58e7
584.3334
(M + H)+
585.3369
292.6727
293.1730
586.3364
100
%
0
100
200
300
400
500
600
700
800
900
1000
1100
1200
1300
1400
1500
1600
1700
1800
1900
m/z

14. ^1H NMR of 2 ($CDCl_3$ 400 MHz):

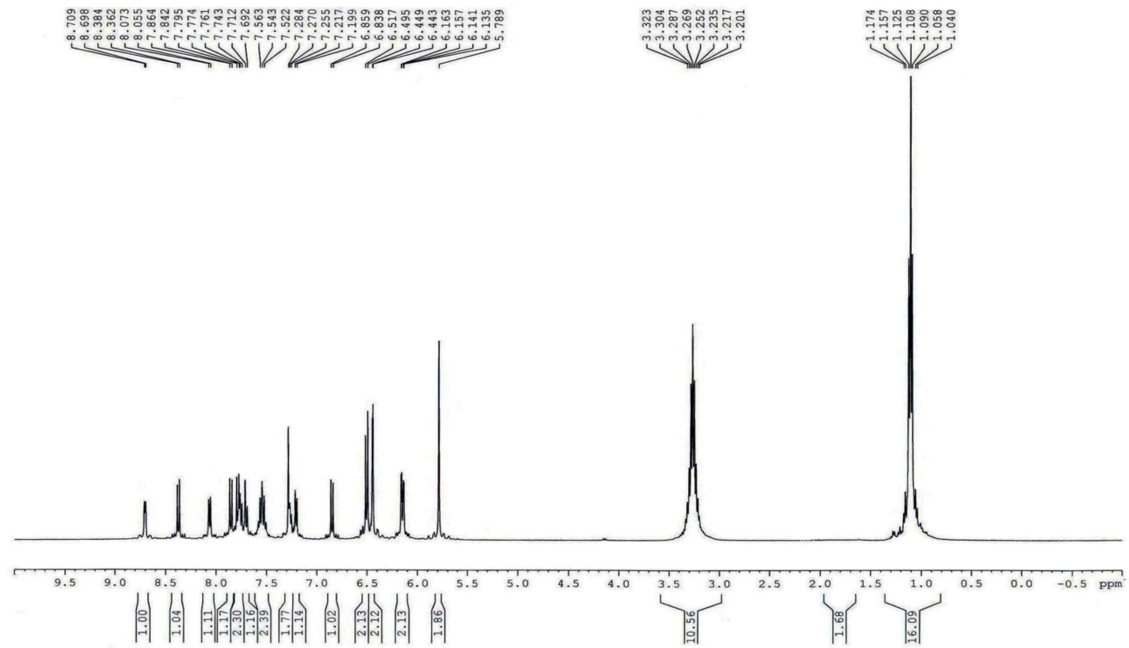

15. ^{13}C NMR of 2 ($CDCl_3$ 100 MHz):

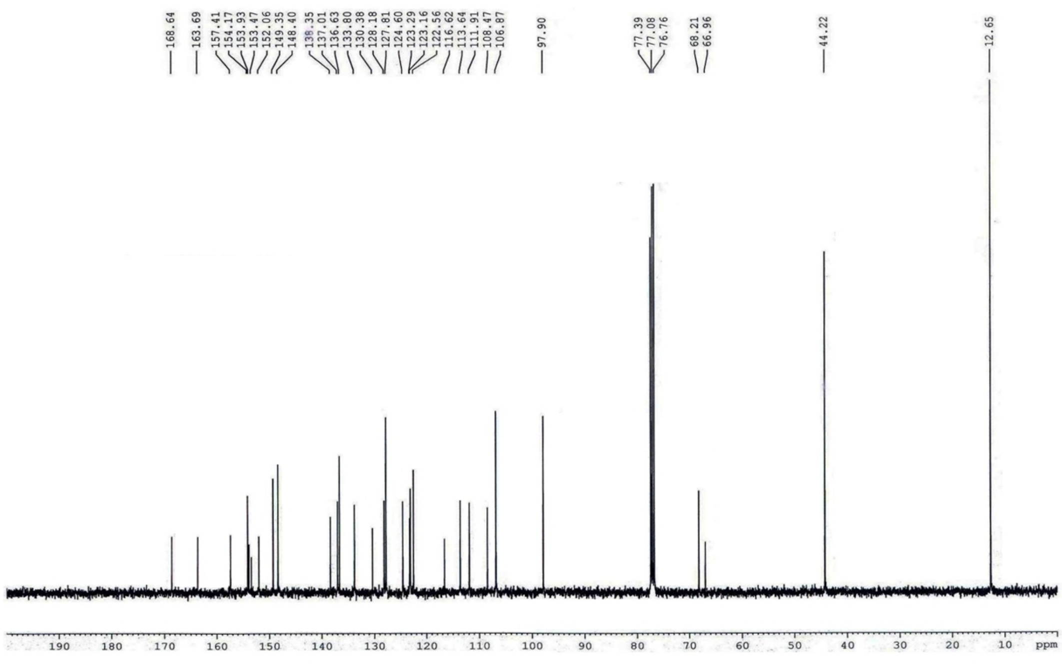

16. Mass of 2:

Reference

1. B. Valeur, J. Pouget, J. Bourson, M. Kaschke and N. P. Eensting, *J. Phys.Chem.*, 1992, **96**, 6545.